EFFECTS OF SIZE AND SLENDERNESS ON DUCTILITY OF FRACTURING STRUCTURES

By Zdeněk P. Bažant,[1] Fellow, ASCE, and Emilie Becq-Giraudon[2]

ABSTRACT: The ductility of an elastic structure with a growing crack may be defined as the ratio of the additional load-point displacement that is caused by the crack at the moment of loss of stability under displacement control to the elastic displacement at no crack at the moment of peak load. The stability loss at displacement control is known to occur when the load-deflection curve of the whole structural system with the loading device (characterized by a spring) reaches a snapback point. Based on the known stress intensity factor as a function of crack length, the well-known method of linear elastic fracture mechanics is used to calculate the load-deflection curve and determine the states of snapback and maximum loads. An example of a notched three-point bend beam with a growing crack is analyzed numerically. The ductility is determined and its dependence of the structure size, slenderness, and stiffness of the loading device is clarified. The family of the curves of ductility versus structure size at various loading device stiffnesses is found to exhibit at a certain critical stiffness a transition from bounded single-valued functions of D to unbounded two-valued functions of D. The method of solution is general and is applicable to cracked structures of any shape. The flexibility (force) method can be adapted to extend the ductility analysis to structural assemblages provided that the stress intensity factor of the cracked structural part considered alone is known. This study leads to an improved understanding of ductility, which should be useful mainly for design against dynamic loads.

INTRODUCTION

Ductility is an important characteristic of the energy absorption capability of a structure under impact, blast, and seismic loads. Ductility of structural parts governs the degree to which overloads can be resisted by redistribution of internal forces.

The growth of a major crack in a structure reduces its ductility. The size as well as the shape of a structure, particularly its slenderness, have a great effect on ductility. Ductility generally decreases as the size of the slenderness increases. This aspect is important for extrapolating to larger sizes the experience gained in laboratory testing or in building structures of normal sizes.

For other than static loads (gravity loads), structures do not fail at the maximum load. Rather, they fail at a certain moment of their postpeak softening. The failure represents a loss of stability, and so the determination of ductility requires stability analysis of a softening structure (Bažant 1976; Bažant and Cedolin 1991, Chapters 12 and 13).

Fracture in the inelastic hinging regions of beams or frames, in the form of either a localized crack or distributed cracking, causes the moment-curvature diagram to exhibit postpeak softening. This invalidates the application of plastic limit analysis, reduces the capacity for energy absorption, and limits the degree of inelastic moment redistribution. The effect of softening in reinforced concrete beams has been analyzed from various viewpoints by a number of investigators [e.g., Schnobrich (1982), Hand et al. (1973), Lin and Scordelis (1975), Maier (1967a,b, 1971a,b), Maier et al. (1973), Mróz (1985), Darvall (1983, 1984), Darvall and Mendis (1985), Warner (1984), and Wood (1968)]. The effect of softening in the inelastic hinging regions of beams on the ductility of statically indeterminate beams and frames on their ductility was studied by layered finite-element analysis (Bažant et al. 1987). Diagrams of structure ductility, defined by a loss of stability, were presented and were shown to depend strongly on the size and shape of structure and, in the case of spring supports, on the stiffness of these supports. In all of these investigations, however, the analysis was limited to the bending theory with the assumption of plane cross sections and with a uniaxial stress-strain relation. Crack propagation was not explicitly considered in those investigations.

The objective of the present paper is use of linear elastic fracture mechanics (LEFM) with an R-curve to analyze ductility of simple elastic structures with a growing crack and thus to obtain diagrams clarifying the dependence of ductility of a cracked structure on its size and slenderness and on the stiffness of the loading system or supports. The cohesive (or fictitious) crack model will not be considered. For that model, an efficient method to calculate the maximum displacement and ductility without having to solve the load-deflection curve was presented by Bažant and Li (1995a,b) are summarized in Bažant and Planas (1998, Section 7.5.5).

DEFLECTION COMPONENTS AND SOFT LOADING

The nonlinear fracture behavior of quasibrittle structures, caused by the fact that the fracture process zone is not negligible compared to specimen dimensions, may be analyzed by means of the equivalent LEFM with an R-curve [e.g., Bažant and Planas (1998, Chapter 5)]

The deflection of a structure with a crack may be expressed as

$$u = u_f + C_0 P \tag{1}$$

where P = applied load (or parameter of a system of loads); u = associated displacement (defined so that $P\,du$ represents the work of load or loads); C_0 = compliance of the structure when there is no crack ($K_0 = 1/C_0$ = stiffness); C_0P = elastic (reversible) part of displacement; and u_f = additional displacement under load P caused by formation of the crack.

Laboratory specimens are normally loaded by a testing machine (or frame) that is never perfectly rigid but has a certain finite stiffness K_m. Thus the actual loading is equivalent to a loading through a spring (Fig. 1) that has some finite stiffness K_m and compliance $C_s = 1/K_m$. Loading for which $C_s > 0$ may be called ''soft'' loading.

Isolating a cracked part from an elastic structure, we may regard it as a cracked substructure elastically restrained by

[1]Walter P. Murphy Prof. of Civ. Engrg. and Mat. Sci., Northwestern Univ., Evanston, IL 60208.

[2]Grad. Res. Asst., Northwestern Univ., Evanston, IL.

Note. Associate Editor: Gilles Pijaudier-Cabot. Discussion open until August 1, 1999. To extend the closing date one month, a written request must be filed with the ASCE Manager of Journals. The manuscript for this paper was submitted for review and possible publication on April 1, 1998. This paper is part of the ***Journal of Engineering Mechanics***, Vol. 125, No. 3, March, 1999. ©ASCE, ISSN 0733-9399/99/0003-0331–0339/$8.00 + $.50 per page. Paper No. 18210.

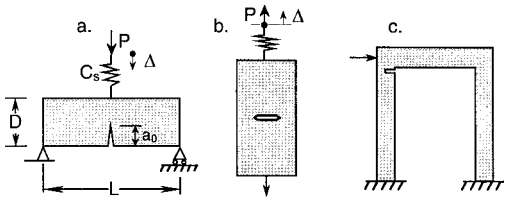

FIG. 1. (a,b) Fracture Specimens Loaded through Spring; (c) Structure with Cracked Part

several springs replacing the action of the remaining crack-free part of the structure. For example, to allow the use of known fracture solutions for beams, the cracked column of the portal frame in Fig. 1(c) may be isolated from the rest of the frame. The restraint by the rest of the frame produces a sort of soft loading. As long as the isolated substructure is statically determinate, the problem is equivalent to our case of loading through a spring. But if a statically indeterminate structure [e.g., the frame in Fig. 1(c)] is analyzed as an assemblage of parts, the problem becomes more complicated because of redistribution of internal forces among structural parts as the crack grows during loading. However, if the energy release function is obtained for the structure as a whole [e.g., the entire portal frame in Fig. 1(c)], the problem becomes identical to the present one.

Structures often contain many cracks. When two or more cracks grow simultaneously, the interaction among the cracks must be analyzed (Bažant and Cedolin 1991), making the problem more complicated than the present one. However, a simultaneous growth of two or more cracks is usually unstable, which causes only one crack to grow while the others unload. Then the problem is again equivalent to the present one.

When a structure is loaded through a spring of nonzero compliance C_s, the total deflection of the structure with the spring is

$$\Delta = u + C_s P = u_f + (C_0 + C_s)P = u_f + C_0(1 + \kappa^{-1})P \quad (2)$$

where $\kappa = K_m/K_0 = C_0/C_s$ = ratio of the stiffnesses of the spring (i.e., the testing machine) and the structure.

The dimension of compliance is length/force. The compliance is inversely proportional to Eb where E = Young's elastic modulus. Because the dimension of Eb is force/length, the compliance must generally have the form

$$C_0 = \frac{f_C(L_1/D,\ L_2/D,\ \ldots)}{Eb} \quad (3)$$

where f_C = dimensionless function and L_1/D, L_2/D, . . . = ratios of various dimensions of the structure to the characteristic dimension D, which characterize the structure shape (geometry) and are constant for geometrically similar structures. Thus C_0 is size independent in the case of two-dimensional similarity (thickness b = constant).

As an example, for the three-point bend beam or the tensioned rectangular strip specimen shown in Figs. 1(a and b)

$$C_0 = \frac{1}{Eb}\left(\frac{L^3}{4D^3} + \frac{3(1+\nu)L}{5D}\right) \quad \text{or} \quad C_0 = \frac{1}{Eb}\frac{L}{D} \quad (4)$$

where ν = Poisson ratio. In the first expression, the first and second terms represent the contributions of bending and shear of the beam. From (3) and (4) it is clear that the compliance of similar crack-free structures is size independent. The ratio L/D characterizes the slenderness of the structure. Obviously, C_0 increases with the slenderness, but this must not be confused with the size effect.

TYPES OF LOAD-DEFLECTION DIAGRAMS AND SNAPBACK

Consider first the diagrams of P versus u_f when the energy release rate is constant, $R(c) = G_f$ = fracture energy of the material. For a zero crack length ($a = 0$), they begin at infinity ($P \to \infty$, Fig. 2), which means that a crack cannot start from a smooth surface according to LEFM. These responses can be of the following two types:

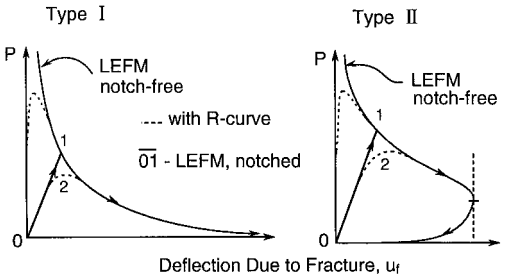

FIG. 2. Two Types of LEFM Fracture Response—without and with Snapback

- Type I, for which the $P(u_f)$-curve always has a negative slope [Fig. 2(a)].
- Type II, for which the slope of the $P(u_f)$-curve reverts at a certain point (called the snapback point) to positive [Fig. 2(b)].

Examples of such curves were given by Bažant (1987) [see also Bažant and Cedolin (1991, Fig. 12.17)]. It can be shown that the type of response is decided by the following criterion:

$$\text{for} \quad \lim_{a \to a_1} \frac{ND}{M} = 0 \quad \text{(Type I)} \quad (5)$$

$$\text{for} \quad \lim_{a \to a_1} \frac{ND}{M} > 0 \quad \text{(Type II)} \quad (6)$$

where a_1 = crack length at the end of the ligament (i.e., when there is a full break); and M and N = bending moment and normal force transmitted across the ligament, respectively.

When the structure has a notch, of length a_0 (or a preexisting traction-free crack), the response first follows a straight line emanating from the origin (lines 01 in Fig. 2), and when the $P(u_f)$-curve for a propagating crack is reached, there is an abrupt slope change. If $R(c)$ varies according to a smooth R-curve, the slope change is not abrupt but rounded (the dashed curves in Fig. 2), and when the R-curve begins with a zero value, a curved diagram begins at the origin and a crack can start even from a smooth surface.

The elastic deflection of the crack-free structure, the additional deflection caused by the crack, and the deflection of the spring are additive. The loads causing these three deflections are the same. Thus, the coupling of the corresponding parts may be imagined as a series coupling (see Fig. 3 where adding the segments a, b, and c on any horizontal line yields the horizontal coordinate $a + b + c$ of the load-deflection curve of the whole system). The inverse slopes (compliances) at the points with the same P (lying on a horizontal line) are also added.

As clarified by Fig. 3, a sufficiently soft spring or a sufficiently soft crack-free structure (i.e., a large enough C_s or C_0) will necessarily cause the total load-deflection diagram to exhibit a snapback (i.e., a point at which the descending response ceases to have a negative slope). If the curve is smooth, it is a point with a vertical tangent ($d\Delta/dP = 0$). This point can represent a point of (locally) maximum deflection, inflexion, or minimum deflection (Fig. 4). The first two cases are known to represent the stability limit under displacement control (Bažant and Cedolin 1991).

For Type I fracture, no vertical tangent nor snapback will occur if the spring and the crack-free specimen are sufficiently stiff (i.e., if C_s and C_0 are small enough). Because an increase

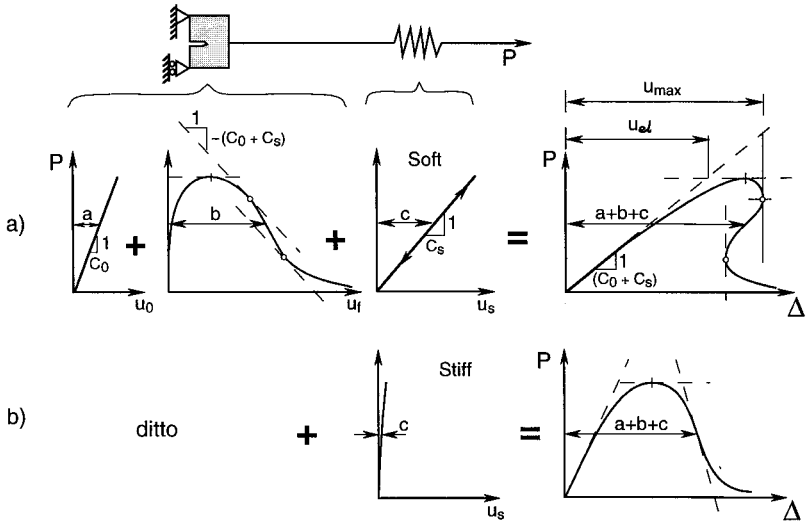

FIG. 3. Superposition of Deflections due to Elasticity of Structure with No Crack (a) and of Spring (c), and Deflection due to Crack (c)

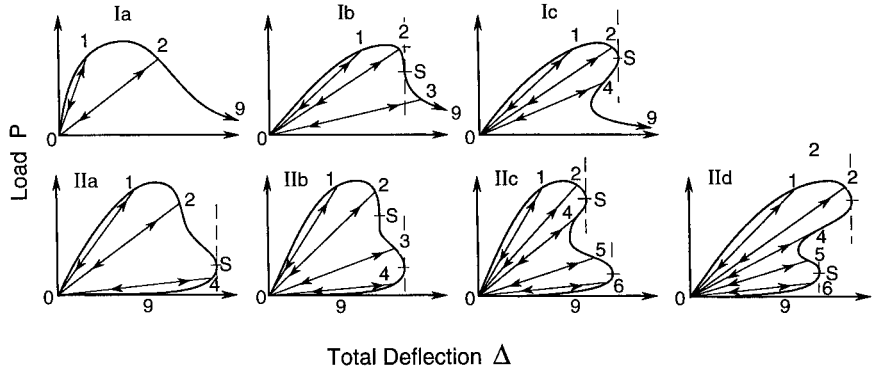

FIG. 4. Various Kinds of Load-Deflection Curves for Crack Growth Characterized by *R*-Curve for Monotonic Loading and Reloading

of slenderness L/D can cause C_0 to exceed any given value, a snapback occurs if (and only if) the structure is sufficiently slender. But this is different for Type II structures, for which a snapback occurs for any slenderness.

From the geometrical construction in Fig. 3, it now transpires that, on the curve of P versus the crack-produced deflection u_f, the point of snapback instability occurs at the point at which the tangent to the curve has the slope $1/C_{cr} = -1/(C_0 + C_s)$ (shown in Fig. 3). From this observation one can readily deduce various Type I or Type II combinations of the $P(u_f)$-curve with the combined elastic deflection characterized by the combined compliance $C_f + C_0$ (the additional effect of the R-curve behavior, which is not shown in Fig. 4, is to ''round off'' the sharp corners on these curves in the manner shown in Fig. 2). These combinations lead to seven different kinds (Ia, . . . , IId) of the overall load-deflection curves $P(\Delta)$, illustrated in Fig. 4. For the types possessing more than one point at which the line of slope $1/C_{cr}$ is tangent, the failure under static displacement-controlled loading will occur at the first such point. However, the shape of the entire $P(\Delta)$-curve is important for dynamic loading. The area enclosed by the $P(\Delta)$-curve, which is the same as the area enclosed by the $P(u_f)$-curve, represents the energy absorption capability of the structure. Maximizing this capability is crucial for the design against seismic, blast, and impact loadings.

If the structure is precracked or notched, the initial loading follows an inclined straight line until the tip of the existing crack or notch becomes critical ($\mathcal{G} = R$); see the line segments 01, 02, 03, . . . in Fig. 4. Thus the load-deflection diagrams can follow any of the paths 019, 029, 039, . . . , 0190, 0290, 0390, . . . identified in Fig. 4. Thus, as seen in Fig. 4, an enormous variety of responses can be encountered in an elastic structure with one growing crack.

DUCTILITY DEFINED BY STABILITY LOSS AT DISPLACEMENT CONTROL

A distinction must be made between material ductility, characterizing the strain at which a plastically yielding material will fail due to a microcrack, and structure ductility. We consider only the latter concept of ductility, which has often been hazy in practice. A rational definition should be based on the stability loss of the structure, as proposed for fracturing or damaging structures in Bažant (1976), and studied in more detail by Bažant et al. (1987). For load control conditions (i.e., for gravity loads), the stability loss occurs when the maximum load is reached.

Ductility is a different concept from the maximum load or strength of the structure. It characterizes the deformation capability under the most stable type of loading, which is the loading under displacement control. In that case, stability is lost at the snapback point (the first point of vertical tangent) of the overall load-deflection curve of the structural system.

Therefore, we define ductility [Fig. 5(a)] as (Bažant 1976)

$$\lambda = \frac{\Delta_{\max}}{\Delta_{el}} = \frac{P_{\text{snap}}(C_0 + C_s + C_f)}{P_{\max}(C_0 + C_s)} \tag{7}$$

where $u_{\max}$ = total deflection of the system (cracked structure with the spring) at the first point of vertical tangent (snapback); P_{snap} = the corresponding load; $P_{\max}$ = maximum load; and Δ_{el} = elastic (reversible) part of the total deflection at maximum load $P_{\max}$ [Fig. 5(a)]. We can say that the ductility is

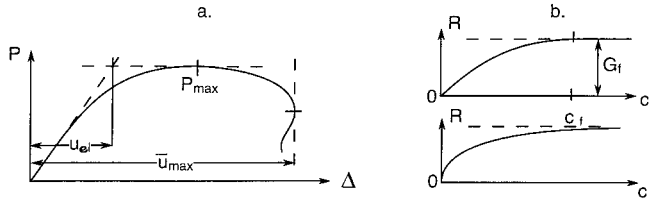

FIG. 5. (a) Definition of Ductility; (b) Two Types of *R*-Curve Considered: $R(c) = G_f\sqrt{cl(c_0 + c)}$ (Upper Curve) and Geometry-Dependent *R*-Curve (Lower Curve)

infinite (or unbounded, $\lambda = \infty$) when no point of vertical tangent exists (as shown in Fig. 4, Case Ia).

Would it make sense to define ductility by some postpeak point with a certain finite-softening slope? It would not. Stability loss does not occur at such a point. If such a finite slope is considered on the load-deflection curve of the structure without the spring, stability loss may of course take place, but such a point must then correspond to a point of vertical tangent on the total load-deflection curve of the system.

Likewise, would it make sense to define ductility by stability loss for the case of soft loading (i.e., real loading for which a perfect displacement control is impossible)? Not at all. A soft loading is equivalent to loading through a spring of a certain nonzero compliance. Even if such a loading is produced electronically, it still is equivalent to a loading through a spring, and such a spring must be considered to be included in the structural system. Moreover, some characteristic value of the loading compliance would have to be chosen completely arbitrarily to define ductility uniquely.

The loss of stability under displacement control, the ductility limit, corresponds in Figs. 2 and 3 to the first point of vertical tangent. For Type Ia in Fig. 4 there is no stability loss under displacement control, which means the ductility is unbounded.

REVIEW OF FRACTURE ANALYSIS OF LOAD-DEFLECTION CURVE

The stress intensity factor K_I and the energy release rate of a crack may be expressed as [e.g., Bažant and Planas (1998)]

$$K_I = \frac{P}{b\sqrt{D}}\, k(\alpha); \quad \mathcal{G} = \frac{K_I^2}{E'} = \frac{P^2}{E'b^2D}\, g(\alpha) \qquad (8a,b)$$

where D = characteristic dimension (size) of the structure; b = thickness of the structure (treated as two-dimensional); $E' = E$ in the case of plane stress (thin structure); $E' = E/(1 - \nu^2)$ in the case of plane strain (thick structure); $g(\alpha) = [k(\alpha)]^2$; $k(\alpha)$ = dimensionless LEFM function that is given for the basic geometries in handbooks (Tada et al. 1985; Murakami 1987) and can be easily determined by elastic finite-element analysis; and

$$\alpha = \frac{a}{D} = \alpha_0 + \Delta\alpha; \quad \alpha_0 = \frac{a_0}{D}; \quad \Delta\alpha = \frac{c}{D}; \quad c = a - a_0 \qquad (9a\text{–}d)$$

where a_0 = length of notch or the traction-free portion of the crack; a = length of the equivalent LEFM crack (up to the tip that lies roughly in the middle of the fracture process zone); and c = length from the notch tip to the tip of the equivalent LEFM crack (which lies roughly in the middle of the fracture process zone).

For notched geometrically similar specimens of different sizes D, α_0 is constant. However, even for notch-free geometrically similar structures, the failure modes are often characterized by approximately constant α_0, within a certain limited size range of practical interest (Bažant and Planas 1998).

For the reader's convenience we now briefly review the well-known calculation of deflection of cracked structure. The energy release rate may also be expressed as

$$\mathcal{G} = \frac{1}{b}\left[\frac{\partial \Pi^*}{\partial a}\right]_P = \frac{1}{b}\frac{\partial}{\partial a}\left[\frac{P^2}{2}\, C(a)\right]_P = \frac{P^2}{2b}\frac{dC(a)}{da} \qquad (10)$$

Substituting (8*b*), one gets $dC(a)/da = 2g(\alpha)/bDE'$. Integration (with initial condition $C = C_0 + C_s$ at $a = 0$) then provides $C(a)$, and the deflection is obtained as $\Delta = C(a)P$. This gives a well-known result [e.g., Bažant and Cedolin (1991) and Bažant and Planas (1998, p. 67)], which may be written as $\Delta = \bar{C}(\alpha)P/b$, from which

$$P = \frac{b\Delta}{\bar{C}(\alpha)} \qquad (11)$$

where

$$\bar{C}(\alpha) = \frac{2}{E'}\,\phi(\alpha) + b(C_0 + C_s); \quad \phi(\alpha) = \int_0^\alpha g(\alpha')\, d\alpha' \qquad (12a,b)$$

At increasing deflection, the crack grows. As it grows, the energy release rate must be equal to its critical value $R(c)$, called the fracture resistance, which may be considered to be a function of the crack extension $c = a - a_0$

$$\mathcal{G} = R(c) \qquad (13)$$

In LEFM, $R(c)$ is assumed to be constant, $R(c) = G_f$. For a quasi-brittle fracture, R must be considered variable, to reflect the gradual development of the fracture process zone. To obtain for notch-free structures realistic load-deflection curves starting from zero (Fig. 2), the R-curve must start from zero. Then it grows at a decreasing rate until, at $c = c_f$, it reaches a certain final value, taken equal to G_f. The R-curve may be considered independent of the structure size D, but it depends on structure geometry (including α_0). Exploiting the known approximate form of the size effect law, one can, for example, determine $R(c)$, including its dependence on the structure geometry, by the size effect method [e.g., Bažant and Planas (1998)].

According to (13) and (8*b*),

$$P^2 = \frac{R(c)}{g(\alpha)}\, E'b^2D; \quad c = D\Delta\alpha \qquad (14a,b)$$

CALCULATION OF DUCTILITY FROM LOAD-DEFLECTION DIAGRAM

For computer programming, it is easier to calculate ductility through numerical evaluation of many points on the load-deflection curve. First we select many closely spaced points $c = c_1, c_2, \ldots$ covering the length of the ligament. We choose, or are given, the values of D, L, κ, and α_0. For each c_i ($i = 1, 2, \ldots$), we evaluate P from (14) and then Δ from (11). Searching among the calculated points (Δ_i, P_i), we determine the point with the first local maximum of Δ and the point with the maximum of P. Refining the subdivision of c_i in the vicinity of these maxima, we can determine the locations of these two maxima with any desired accuracy. The ductility for the given values of D, L, κ, and α_0 is then evaluated from (7).

This approach works even if the peak or the snapback is pointed.

DUCTILITY BY MEANS OF DIRECT CALCULATION OF MAXIMUM POINTS

Maximum Load

In this case, the energy balance condition $\mathcal{G} = R(c)$ must remain satisfied after an infinitesimal crack length increment at constant P. Therefore, as long as the load-deflection curve is smooth (i.e., cases such as vertex 2 in Fig. 2 or vertex 4 in

Fig. 4 are excluded), the maximum load (peak) is characterized by the condition

$$\left[\frac{\partial \mathcal{G}}{\partial a}\right]_P = R'(c) \tag{15}$$

Substituting (8*b*) into (13) and (15), we obtain two conditions

$$P^2 = \frac{E'b^2D}{g(\alpha)} R(c); \quad P^2 = \frac{E'b^2D^2}{g'(\alpha)} R'(c) \tag{16a,b}$$

where the primes denote the derivatives of the functions. Dividing now the second of the last two equations by the first, we get the maximum load condition

$$D = \frac{R(c)g'(\alpha)}{R'(c)g(\alpha)}; \quad \alpha = \alpha_0 + \frac{c}{D} \tag{17a,b}$$

Maximum Displacement

First we must express $\mathcal{G}$ in terms of the total displacement. To this end, we substitute (12) into (8*b*) getting

$$\mathcal{G} = \frac{E'}{D} \Delta^2 \psi(\alpha) \tag{18}$$

in which we denoted

$$\psi(\alpha) = \frac{g(\alpha)}{[2\phi(\alpha) + E'b(C_0 + C_s)]^2} \tag{19}$$

Assuming again a smooth curve, the energy balance condition $\mathcal{G} = R(c)$ at maximum displacement must remain satisfied after an infinitesimal crack length increment at constant u. Therefore, the point of maximum displacement (snapback) is characterized by the condition

$$\left[\frac{\partial \mathcal{G}}{\partial a}\right]_\Delta = R'(c) \tag{20}$$

This condition means that, at maximum displacement, the $\mathcal{G}(a)$-curve is tangent to the R-curve. Substituting (18) into (13) and into (20), we obtain two conditions

$$\Delta^2 = \frac{D}{E'} \frac{R(c)}{\psi(\alpha)}; \quad \Delta^2 = \frac{D^2}{E'} \frac{R'(c)}{\psi'(\alpha)} \tag{21a,b}$$

Dividing now the second of these two equations by the first, we get the maximum load condition

$$D = \frac{R(c)\psi'(\alpha)}{R'(c)\psi(\alpha)}; \quad \alpha = \alpha_0 + \frac{c}{D} \tag{22a,b}$$

The relationship of the $\mathcal{G}(a)$ and $R(c)$ may be clarified by the same kind of argument as for the case of controlled load P [e.g., Bažant and Planas (1998) and Bažant et al. (1986)]. Fig. 6(a) shows the curves of $\mathcal{G}(a)$ for a given size D and an increasing succession of constant displacement values $\Delta = \Delta_1$, $\Delta = \Delta_2$, . . .). The fracture equilibrium states are the intersections of these curves with the R-curve. The first intersection point on each curve is a stable state [because $R'(c) > \mathcal{G}'(a)$], and the second one is an unstable state. From this picture, it is clear that the limit of stability (i.e., failure) occurs for the $\Delta = \Delta_{max}$, for which $\mathcal{G}'(a) = R'(c)$, as already stated in (20). When different sizes $D = D_1, D_2, D_3, \ldots$ are considered, a different value $\Delta_{max,i}$ (i = 1, 2, 3. . .) corresponds to each size. The curves of $\mathcal{G}(a)$ at $\Delta = \Delta_{max,i}$ for various D_i must all be tangent to the R-curve, as shown in Fig. 6(b). In other words, the R-curve is an envelope of the $\mathcal{G}(a)$ curves at Δ = constant for various sizes (and could in fact be determined in that manner). The envelope property is the same as for the $\mathcal{G}(a)$ at constant load P for different sizes (Bažant et al. 1986).

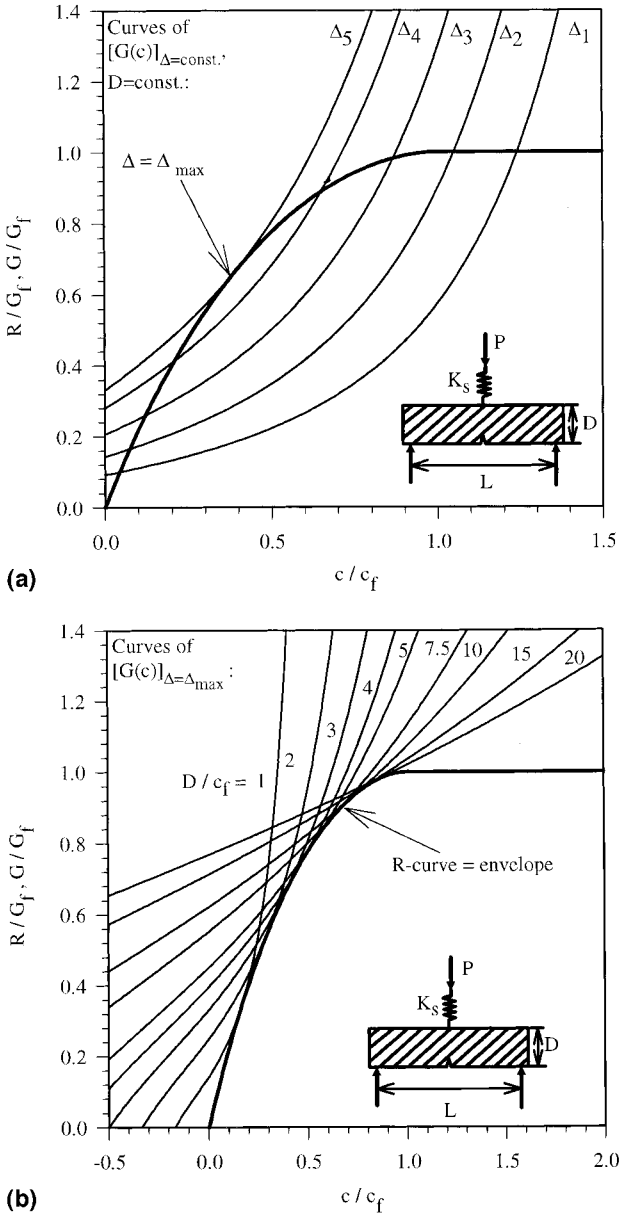

FIG. 6. (a) Graphic Determination of Maximum Displacement from Tangent Point to *R*-Curve and Energy Release Curve; (b) *R*-Curve as Envelope of Energy Release Rates at Maximum Displacement for Various Characteristic Sizes (Displacement Control)

Computation Procedure

With the foregoing formulation, which is feasible only if the snapback and the peak are smooth, it is not necessary to calculate the entire load-deflection curve. But it is convenient to obtain the ductility values simultaneously for the whole range of D-values (or, in a similar manner, for the whole range of values of L/D, κ, and α_0). We choose a series of discrete values $c_{snap} = c_1, c_2, \ldots$ covering the length of the ligament. For each of them we evaluate D from (22), and then we evaluate $\Delta = \Delta_{max}$ for the snapback point from one of the equations [(21)]. Then, for each calculated value of D we solve $c = c_{max}$ from the nonlinear equation (17) (e.g., by Newton iterative method). Finally we evaluate $\Delta_{el} = (C_0 + C_{el})P_{max}$ and the ductility from (7). Obviously, the solution of a nonlinear equation cannot be avoided in this approach.

NUMERICAL STUDY AND SHAPE OF DUCTILITY DIAGRAMS

The main purpose of this study is to determine the shape of the diagrams describing how ductility depends on the structure size, spring stiffness, and slenderness. To this end, numerical calculations are carried out for the case of a notched three-point bent beam shown in Fig. 1(a), for which the $P(\Delta)$-curve is known to be of Type I (Fig. 2).

The fracture properties are considered the same as previously determined in the testing of concrete and limestone (Bažant and Pfeiffer 1987; Bažant et al. 1991). The notch depth is $a_0 = D/6$ in the case of concrete, and $a_0 = 0.4D$ in the case of limestone. For the diagrams of ductility versus beam size, the span-to-depth ratio is taken as 2.5 for concrete and 4 for limestone. The material is assumed to follow an *R*-curve beginning with a zero value of energy release rate. Two different types of *R*-curve are considered: (1) An *R*-curve given by

$$R(c) = G_f \sqrt{\frac{c}{c_0 + c}} \tag{23}$$

which starts with a vertical tangent [Fig. 5(b), lower diagram] [c_0 = material constant taken equal to 25.4 mm (1 in.)]; and (2) the size effect *R*-curve [Fig. 5(b), upper diagram] proposed by Bažant and Kazemi (1990) [see also Bažant and Cedolin (1991), Eqs. 12.3.7–12.3.8], which starts from zero with an inclined tangent. This *R*-curve does not have a closed-form expression but is given parametrically by two explicit equations, which involve two material parameters, G_f and c_f. The former *R*-curve gives similar behavior as an *R*-curve starting with an inclined tangent from a finite initial value.

Figs. 7(a and b) and 8(a and b) show, in doubly logarithmic scales, the calculated diagrams of ductility of geometrically similar beams as a function of the beam size *D*, for concrete and limestone, respectively. To present the numerical results in the greatest possible generality, we need to express them in a dimensionless form. The ductility λ is dimensionless, and the size *D* is nondimensionalized by using as a parameter the relative size D/D_0, where $D_0 = c_f g(\alpha_0)/g'(\alpha_0)$ represents the transitional size of Bažant's size effect law $\sigma_N = Bf'_t/\sqrt{(1 + D/D_0)}$, where σ_N is the nominal strength of the

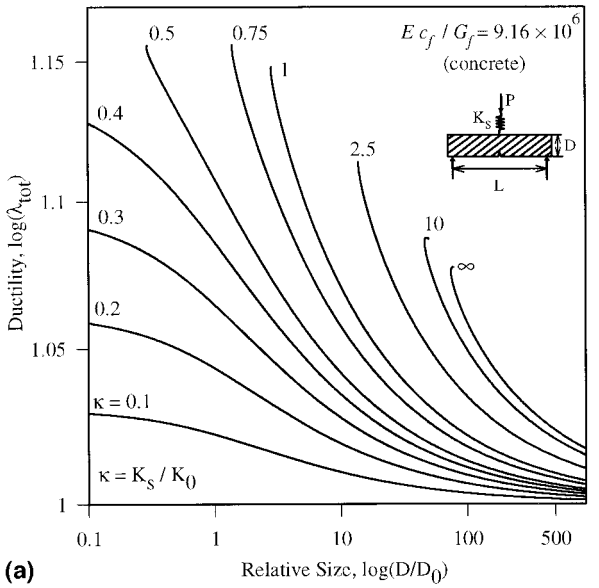

(a)

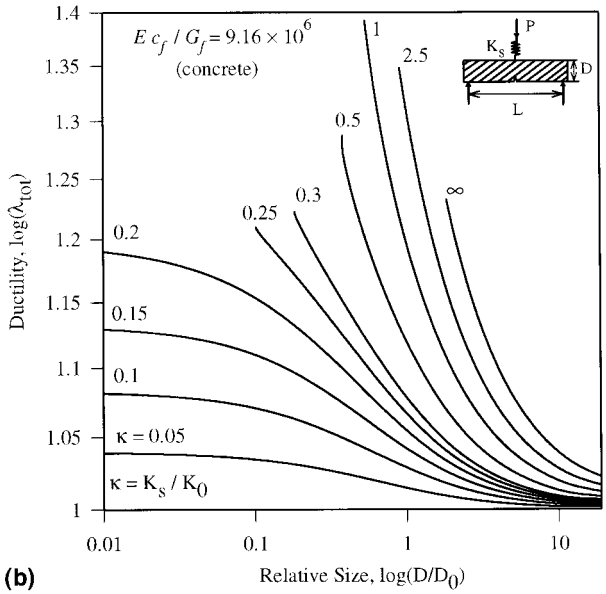

(b)

FIG. 7. Ductility of Concrete versus Specimen Size in Double Logarithmic Plot, Obtained for Two Types of *R*-Curve Considered: (a) $R(c) = G_f\sqrt{c/(c_0 + c)}$; (b) Geometry-Dependent *R*-Curve

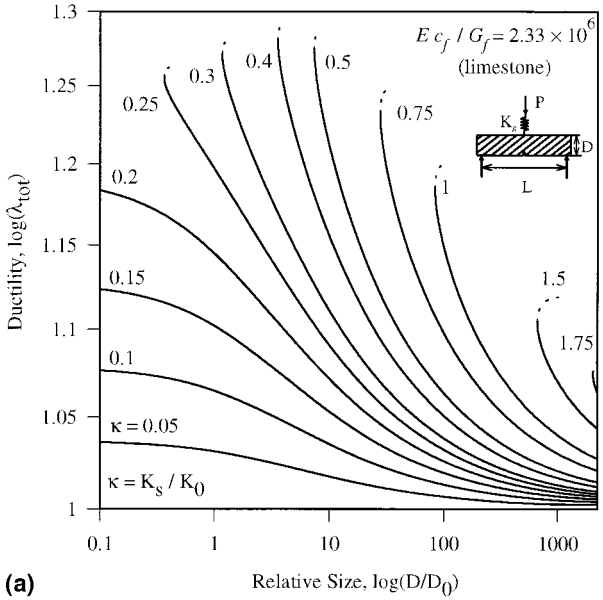

(a)

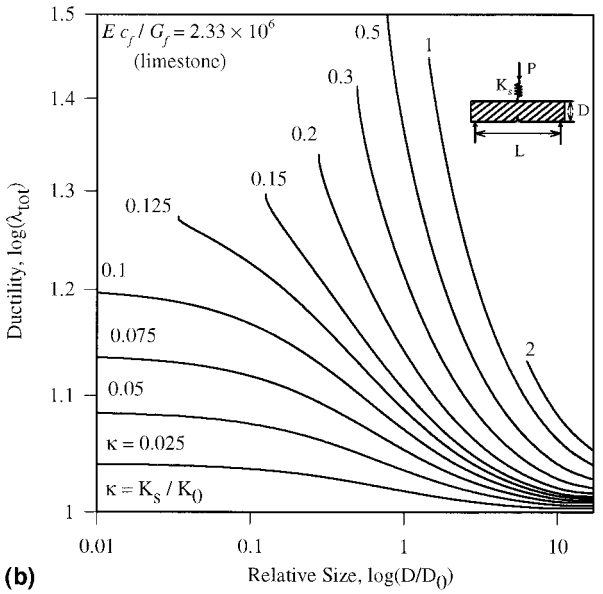

(b)

FIG. 8. Ductility of Limestone versus Specimen Size in Double Logarithmic Plot, Obtained for Two Types of *R*-Curve Considered: (a) $R(c) = G_f\sqrt{c/(c_0 + c)}$; (b) Geometry-Dependent *R*-Curve

structure, B is an empirical coefficient, and f_u is a measure of tensile strength.

If R-curves are used, the solution depends only on three material characteristics: G_f, c_f, and E, whose metric dimensions are N/m, m, and N/m^2. According to Buckingham's theorem of dimensional analysis, the number of governing parameters equals the number of all parameters minus those of independent dimensions. Because N/m^2 = (N/m)/m, we have only two independent dimensions, N/m and m, and so we know there is only one independent dimensionless material parameter. We choose it as $\theta = Ec_f/G_f$. The diagrams are plotted for various values of the relative spring stiffness, characterized by the ratio $\kappa = K_s/K_0 = C_0/C_s$.

From Figs. 7 and 8, we see that the diagrams of ductility versus relative beam size D/D_0 cover the entire range of sizes D/D_0 only if the relative spring stiffness is sufficiently small. The reason is that, for a high enough spring stiffness, the load-deflection diagram exhibits no snapback. That this can happen is clear by comparing the geometrical constructions in Figs. 3(a and b). As a consequence, the family of the ductility curves for various spring stiffnesses exhibits a transition from bounded single-valued functions of D/D_0 to unbounded functions of D/D_0. The critical size $(D/D_0)_{cr}$ below which there is no snapback is a characteristic property of the beam. Note that, in the case of concrete, the entire range of spring stiffness is covered for high beam sizes, whereas, in the case of limestone, ductility is not defined for a spring parameter exceeding 2. In the latter case, the load-deflection diagram does not exhibit snapback beyond a certain value of the spring stiffness.

For some of the curves in Figs. 7 and 8 that have a point of vertical tangent, one has two ductility values for the same D/D_0-value. [This is particularly obvious in the case of limestone for $R(c) = G_f\sqrt{c/(c + c_0)}$.] They correspond to the first and second point of vertical tangent on the curve $P(\Delta)$ in Fig. 3(a). Because stability is lost at the first such point (snapback point), only that point is relevant to failure. Therefore, ductility is indicated by the lower branch of the curve of λ versus D/D_0, lying below the point of vertical tangent in Figs. 7 and 8. The upper branch represents the states of stability restoration rather than stability loss.

Figs. 9(a and b) and 10(a and b) show, in semilogarithmic plots, similar diagrams for various spans characterized by the beam slenderness L/r and two relative spring stiffness values;

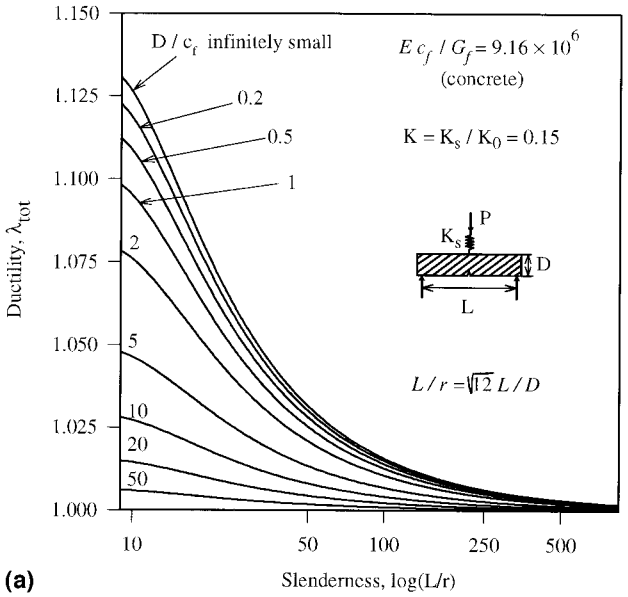

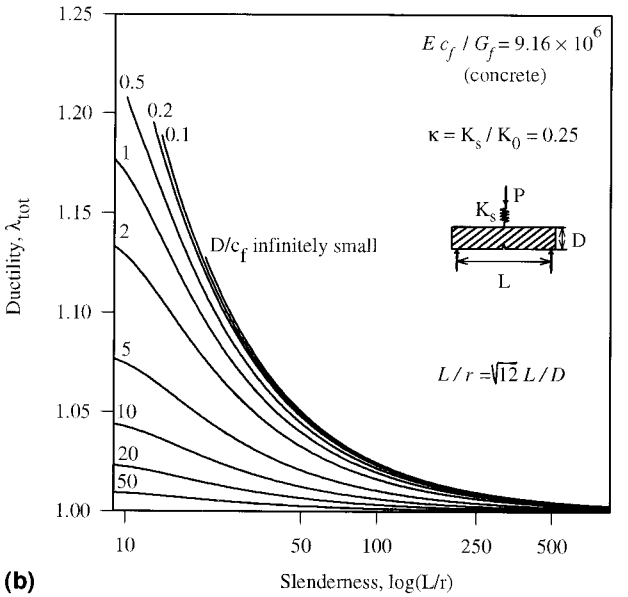

FIG. 9. Ductility of Concrete versus Slenderness in Semilogarithmic Plot, Obtained for Geometry-Dependent *R*-Curve: (a) κ = 0.15; (b) κ = 0.25

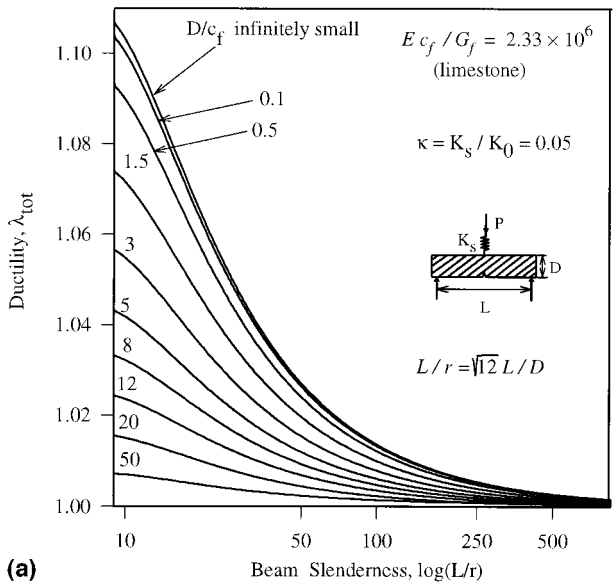

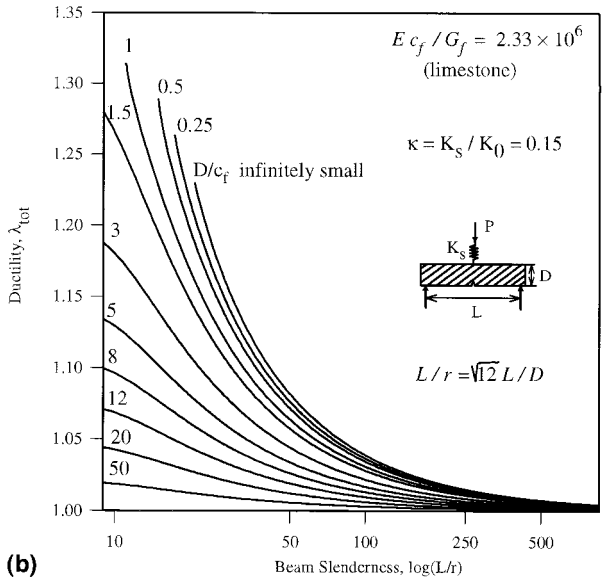

FIG. 10. Ductility of Limestone versus Slenderness in Semilogarithmic Plot, Obtained for Geometry-Dependent *R*-Curve: (a) κ = 0.1; (b) κ = 0.15

L = span; $r = D/\sqrt{12}$ = radius of gyration of a rectangular cross section of the beam; $L/r = \sqrt{12}L/D$. The typical fracture characteristics of concrete and limestone are considered. The diagrams are calculated for a span-to-depth ratio varying from 2.5 to 250. Figs. 9 and 10 show that the ductility decreases with increasing slenderness quite rapidly.

One can also observe that these diagrams depend on the spring parameter. For instance, for the properties of concrete and $\kappa = 0.15$, there is a finite ductility for every beam size [Fig. 9(a)], whereas for $\kappa = 0.25$, the ductility is unbounded for any beam size [Fig. 9(b)] (which means that the load-deflection diagram cannot exhibit snapback). The same observation can be made in the case of limestone [compare Figs. 10(a and b)]. The ductility diagrams lie above the line $\lambda = 1$ and are bounded from above by a certain limit curve, which depends on the spring stiffness parameter κ. This bounding diagram is approached for very small beam sizes $D \to 0$.

OTHER STRUCTURE TYPES AND THREE-DIMENSIONAL SIMILARITY

Although a calculation example has been presented only for the three-point bend beam, the method of analysis given by (1)–(22) is completely general and is applicable to any type of structures for which the dimensionless function $k(\alpha)$ characterizing the stress intensity factor is known.

The case of cracked structures similar in three dimensions, such as axisymmetric specimens with a radially growing circular crack, can be analyzed similarly, and the results are qualitatively the same. In that case, the uncracked compliance $C_0 \propto 1/D$, but the size dependence of C_0 is compensated by the fact that the length of the fracture front is proportional to D.

In the case of one-dimensional similarity, such as the ease of a tensioned bar with a cohesional crack or damage zone opening simultaneously over the entire cross section [which has been analyzed in Bažant (1976)], the size effect becomes the same as the slenderness effect, and the behavior is qualitatively the same as the slenderness effect described here.

GENERALIZATION TO COMPLEX STRUCTURES WITH CRACKED PARTS

Consider now structures of various sizes representing an assemblage of parts, for example, beams, one of which contains a large growing crack. One way to calculate the ductility of such a structure is to obtain function $k(\alpha)$ or $\mathcal{G}(\alpha)$ for the entire structure, by the brute force approach of finite elements. But in such an approach the entire fracture analysis needs to be repeated for each structure size or slenderness and does not explicitly reveal the effect of size, slenderness, or other shape changes in the elastic structure adjoining the structural part.

A simpler, more instructive, and more general way, which makes the effects of size, slenderness, and shape conspicuous and does not require repeating fracture analysis for each case, is to apply the flexibility (or force) method for structural assemblages, which are, in general, statically indeterminate. The calculation may proceed in a similar manner as that illustrated for the simple assemblage of cracked beam and spring.

Let F_i ($i = 1, 2, \ldots, n$) be the generalized internal forces (such as bending moments, normal forces, and shear forces) by which the isolated cracked structural part (e.g., the cracked beam in Fig. 11) interacts with the rest of the structure. The structure obtained by severing the connections that transmit F_i will be called the primary structure. Further let Δ_i be the associated generalized displacements (e.g., relative rotations, relative normal, or shear displacement) of the whole primary structure, such that $F_i d\Delta_i$ be the correct expressions for work, and Δ be the displacement associated with P. Denote C_{ij}^{el},

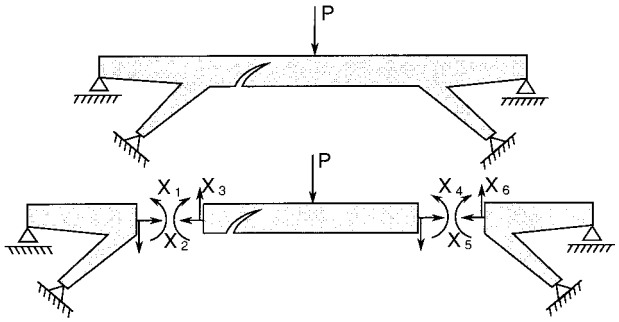

FIG. 11. Cracked Structural Part Isolated from Complex Structure

$C_i^{el,P}$, and $C^{el,PP}$ = elastic compliances representing deflections in the sense of Δ_i due to $F_j = 1$ and to load $P = 1$ for the whole primary structure when the isolated structural part has no crack. Further denote $C_{ij}^{fr}(a)$, $C_i^{fr,P}(a)_i$, and $C^{fr,PP}(a)$ = additional compliances of the isolated cracked structural part alone, caused by a crack of length a (these need to be determined by the fracture mechanics method of the type already described). Then, in a matrix form, the total generalized displacements are

$$\{\Delta_i\} = [C_{ij}]\{F_j\} + \{C_i^P\}P; \quad \Delta = \{C_i^P\}^T\{F_i\} + C^{PP}P \qquad (24a,b)$$

where

$$C_{ij} = C_{ij}^{el} + C_{ij}^{fr}(a); \quad C_i^P = C_i^{el,P} + C_i^{fr,P}(a) \qquad (25a,b)$$

$$C^{PP} = C^{el,PP} + C^{fr,PP}(a) \qquad (25c)$$

represent the total compliances of the whole primary structure due to both elasticity and fracture.

Compatibility requires that $\Delta_i = 0$. Then, solving the first matrix equation in (24) for F_j and substituting it into the second, we obtain

$$\Delta = (C^{PP} + \{C_i^P\}^T[C_{ij}]^{-1}\{C_j^P\})P \qquad (26)$$

The advantage gained by this formulation is that, if the rest of the structure is changed arbitrarily while the cracked part is only scaled in size but does not change its shape, one can dispense with repeating the fracture mechanics analysis of the cracked part. A whole range of solutions for structures with different slendernesses or shapes of the crack-free parts can be readily obtained.

SUMMARY AND CONCLUSIONS

1. The ductility, conceived in the sense of stability limit, may be defined as the ratio of the fracturing displacement at the limit of stability under displacement control to the elastic part of displacement at maximum load. An example of a notched three-point bend beam with a growing crack has been analyzed numerically. The ductility has been determined, and its dependence on the structure size, slenderness, and stiffness of the loading device has been clarified.
2. The family of the curves of ductility versus relative structure size at various loading device stiffnesses or various slendernesses is found to exhibit, at a certain critical size, a transition from bounded single-valued functions of size to unbounded two-valued functions of size.
3. The flexibility (force) method can be adapted to analyze the ductility of structural assemblages. To this end, it is necessary and sufficient to know the stress intensity factor of the cracked structural part considered separately.

ACKNOWLEDGMENTS

Partial financial support under National Science Foundation grant CMS-9713944 and additional support from the ACBM center at Northwestern University is gratefully acknowledged.

APPENDIX. REFERENCES

Bažant, Z. P. (1976). ''Instability, ductility, and size effect in strain-softening concrete.'' *J. Engrg. Mech. Div.*, ASCE, 102(2), 331–344.
Bažant, Z. P. (1987). ''Snapback instability at crack ligament tearing and its implication for fracture micromechanics.'' *Cement and Concrete Res.*, 17, 951–967.
Bažant, Z. P. (1988). ''Stable states and paths of structures with plasticity or damage.'' *J. Engrg. Mech.*, ASCE, 114(12), 2013–2034.
Bažant, Z. P., and Cedolin, L. (1991). *Stability of structures: elastic, inelastic, fracture and damage theories*. Oxford University Press, New York.
Bažant, Z. P., Gettu, R., and Kazemi, M. T. (1991). ''Identification of nonlinear fracture properties from size effect tests and structural analysis based on geometry-dependent *R*-curves.'' *Int. J. Rock Mech. Mat. Sci. & Geomech. Abstr.*, 28(1), 43–51.
Bažant, Z. P., and Kazemi, M. T. (1990). ''Determination of fracture energy, process zone length and brittleness number from size effect, with application to rock and concrete.'' *Int. J. Fracture*, 44, 111–131.
Bažant, Z. P., Kim, J. K., and Pfeiffer, P. A. (1986). ''Nonlinear fracture properties from size effect tests.'' *J. Struct. Engrg.*, ASCE, 112, 289–307.
Bažant, Z. P., and Li, Y.-N. (1995a). ''Stability of cohesive crack model: Part I—Energy principles.'' *J. Appl. Mech.*, 62(Dec.), 959–964.
Bažant, Z. P., and Li, Y.-N. (1995b). ''Stability of cohesive crack model: Part II—Eigenvalue analysis of size effect on strength and ductility of structures.'' *J. Appl. Mech.*, 62(Dec.), 965–969.
Bažant, Z. P., and Pfeiffer, P. A. (1987). ''Determination of fracture energy from size effect and brittleness number.'' *ACI Mat. J.*, 84, 463–480.
Bažant, Z. P., Pijaudier-Cabot, G., and Pan, J.-Y. (1987). ''Ductility, snapback, size effect and redistribution in softening beams and frames.'' *J. Struct. Engrg.*, ASCE, 113(12), 2348–2364.
Bažant, Z. P., and Planas, J. (1998). *Fracture and size effect in concrete and other quasibrittle materials*. CRC, Boca Raton, Fla., and London.
Darvall, P. LeP. (1983). ''Critical softening of hinges in indeterminate beams and portal frames.'' *Civ. Engrg. Trans.*, 25(3), I. E. Australia, Clayton, Australia, 199–210.
Darvall, P. LeP. (1984). ''Critical softening of hinges in portal frames.'' *J. Struct. Engrg.*, ASCE, 110(1), 157–162.
Darvall, P. LeP. (1985). ''Elastic-plastic-softening analysis of plane frame.'' *J. Struct. Engrg.*, ASCE, 114(4), 871–888.
Hand, F. R., Pecknold, D. A., and Schnobrich, W. C. (1973). ''Nonlinear layered analysis of RC plates and shells.'' *J. Struct. Div.*, ASCE, 99(7), 1491–1505.
Lin, C. S., and Scordelis, A. (1975). ''Nonlinear analysis of RC shells of general form.'' *J. Struct. Div.*, ASCE, 101(3), 523–538.
Maier, G. (1967a). ''On elastic-plastic structures with associated stress-strain relations allowing for work softening.'' *Meccanica*, 2(1), 55–64.
Maier, G. (1967b). ''Extremum theorems for the analysis of elastic plastic structures containing unstable elements.'' *Meccanica*, 2(1), 55–64.
Maier, G. (1971a). ''On structural stability due to strain-softening.'' *Proc., IUTAM Symp. on Instability of Continuous Sys.*, Springer, Berlin, 411–417.
Maier, G. (1971b). ''Incremental plastic analysis in the presence of large displacements and physical instabilizing effects.'' *Int. J. of Solids and Struct.*, 7, 345–372.
Maier, G., Zavelani, A., and Dotreppe, J. C. (1973). ''Equilibrium branching due to flexural softening.'' *J. Engrg. Mech. Div.*, ASCE, 99(4), 897–901.
Mróz, Z. (1985). ''Current problems and new directions in mechanics of geomaterials.'' *Mechanics of geomaterials: Rocks, concretes, soils*, Z. P. Bažant, ed., Chapter 24, Wiley, Chichester, England, and New York, 534–566.
Murakami, Y. (1987). *Stress intensity factors handbook*. Pergamon, London.
Schnobrich, W. C. (1982). ''Concrete cracking.'' *Finite element analysis of reinforced concrete (state-of-the-art report)*, Chapter 4, ASCE, New York, 204–233.
Tada, H., Paris, P. C., and Irwin, G. R. (1985). *The stress analysis of cracks handbook*, 2nd Ed., Paris Productions, Inc., St. Louis.
Warner, R. F. (1984). ''Computer simulation of the collapse behavior of concrete structures with limited ductility.'' *Proc., Int. Conf. Comp.-Aided Analysis and Des. of Concrete Struct.*, F. Damjanic, E. Hinton, et al., eds., Pineridge, Swansea, U.K., 1257–1270.
Wood, R. H. (1968). ''Some controversial and curious developments in the plastic theory of structures.'' *Engineering plasticity*, J. Heyman and F. A. Leckie, eds., Cambridge University Press, Cambridge, England, 665–691.